Stable Continuous-Wave Lasing from Discrete Cesium Lead Bromide Quantum Dots embedded in a Microcavity

Hongbo Zhang[#a], Wen Wen[#a], Bowen Du[#ac], Lei Zhou[e], Yu Chen[af], Shun Feng[ag], Chenji Zou[a], Lishu Wu[a], Hong Jin Fan[a], Weibo Gao[a], Handong Sun*[a], Jingzhi Shang*[d], Ting Yu*[b]

a. Division of Physics and Applied Physics, School of Physical and Mathematical Sciences, Nanyang Technological University, Singapore 637371, Singapore.

b. School of Physics Science and Technology, Wuhan University, Wuhan 430072, People's Republic of China.

Wuhan Institute of Quantum Technology, Wuhan 430206, China

c. College of Physics and Optoelectronic Engineering, Shenzhen University, Shenzhen 518060, China.

d. Shaanxi Institute of Flexible Electronics (SIFE), Northwestern Polytechnical University (NPU), Xi'an, 710129, China

e. School of Chemical Engineering and Technology, Sun Yat-Sen University, Zhuhai 519082, PR China.

f. Commonwealth Scientific and Industrial Research Organisation (CSIRO) Manufacturing, Clayton, Victoria 3168, Australia

g. Institute of Photonics and Quantum Sciences, SUPA, Heriot-Watt University, Edinburgh EH14 4AS, UK

Figure S1 Spatial emission properties of as-fabricated $CsPbBr_3$ QD VSCEL.

Figure S2 FDTD simulation for reflection spectrum with the perpendicular incidence.

Figure S3 PL measurement at 80 K.

Figure S4 Lasing characterization of $CsPbBr_3$ QDs VSCEL after one-year preservation.

Figure S5 Photoluminescence spectra and their fitting curves by Voigt function.

Figure S6 AFM image of $CsPbBr_3$ QDs spin-coated on DBRs.

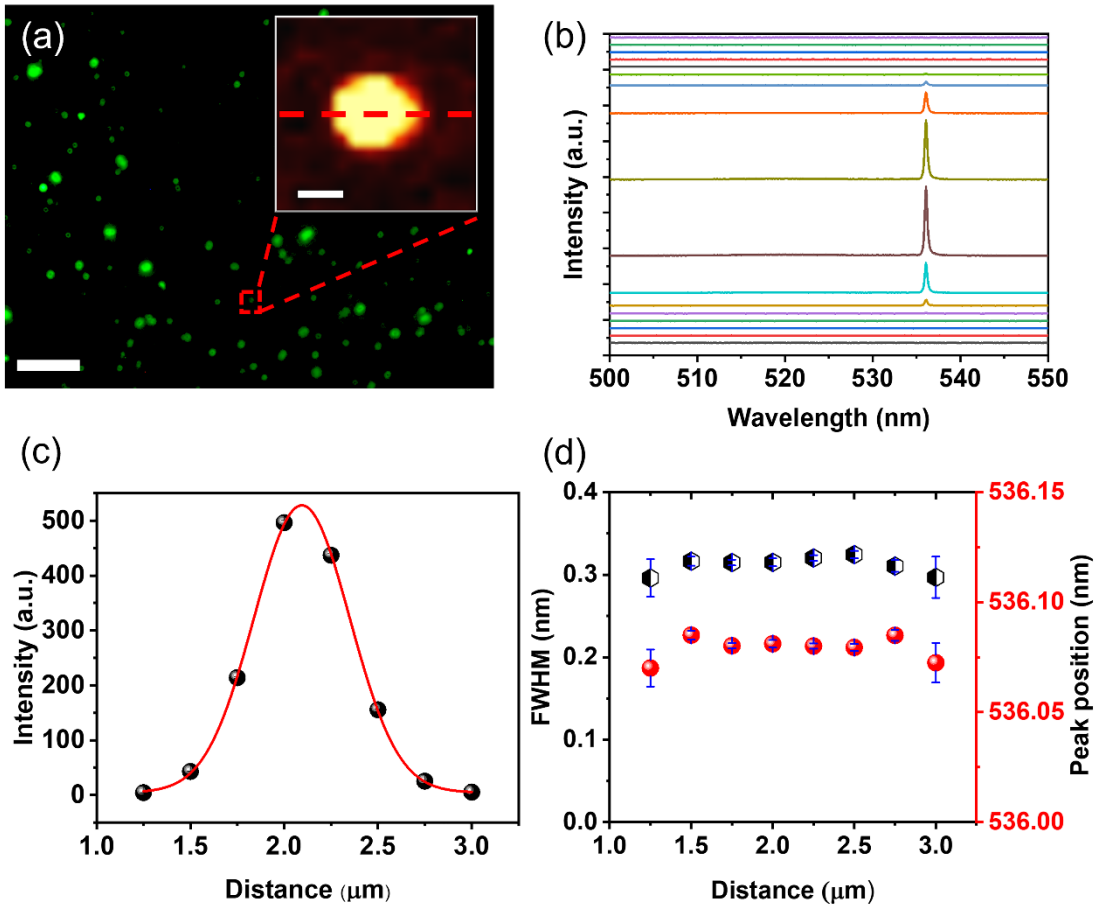

Figure S1 Spatial emission properties of as-fabricated $CsPbBr_3$ QD VSCEL. (a) Fluorescence image of fabricated $CsPbBr_3$ QDs embedded microcavity. Scale bar: 15 μm. Inset: PL intensity mapping image of the microcavity sample, which is collected from the marked region. Scale bar:500 nm. (b) PL spectra collected across the labeled line with a small step of 250 nm. The color traces from bottom to top stand for the spectra taken from left to right along the red dash line in the insert of (a). (c)-(d)The intensity, line width, and peak position of PL emission across the labeled line from left to right, respectively. The solid line in (c) is a fitting curve with a Gaussian function.

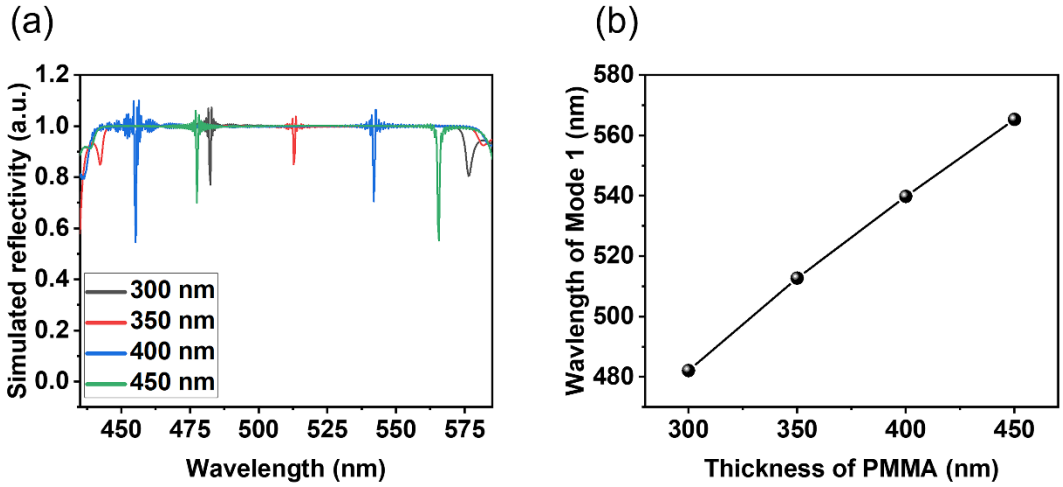

Figure S2 (a) Simulated reflection spectra of cavities with various thicknesses. (b) Wavelength of Mode 1 (i.e., the resonance mode in the longer wavelength) as a function of the thickness of PMMA.

As a Fabry-Pérot microcavity, the cavity length between two DBRs is designed as

$$L = N\frac{\lambda}{2n_c}$$

where N is a positive integer, λ is the optical wavelength, n_c is the effective group index of the cavity.

Here, the PMMA layer works as the spacer inside the cavity and controls the cavity length. As shown in Fig S2a, the cavities constructed by various PMMA thicknesses of 300, 350, 400, and 450 nm support resonances at 482.1, 512.7, 540.1, and 565.3 nm, respectively. These modes are denoted as mode 1. The cavities constructed by the PMMA thicknesses of 400 and 450 nm also show resonances at 455.3 and 477.7 nm, but they are out of the PL emission range of $CsPbBr_3$ QDs, noted as mode 2. The wavelength of resonance mode 1 increases linearly with the cavity wavelength (Fig S2b), which is consistent well with the theoretical Fabry-Pérot resonance. The cavity length with 400 nm PMMA is chosen because it exhibits a resonance mode at 540.1 nm

(blue curve in Fig S2a), which is well overlapped with the gain spectrum of perovskite material (i.e., the lower energy side of the emission range). This spectral overlap enables the strong confinement of PL emission, optical gain, and establishment of lasing.

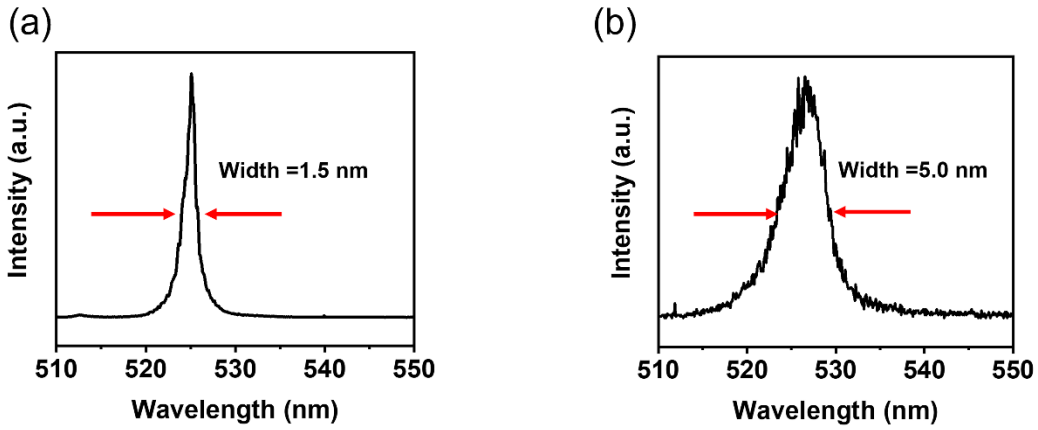

Figure S3 PL measurement at 80 K. (a) PL spectrum of the isolated $CsPbBr_3$ QDs, which is diluted to the same concentration used for $CsPbBr_3$ VCSEL. (b) PL spectrum of the high-density ensembles of $CsPbBr_3$ QDs, which is 10 times of the concentration of the $CsPbBr_3$ QDs in (a).

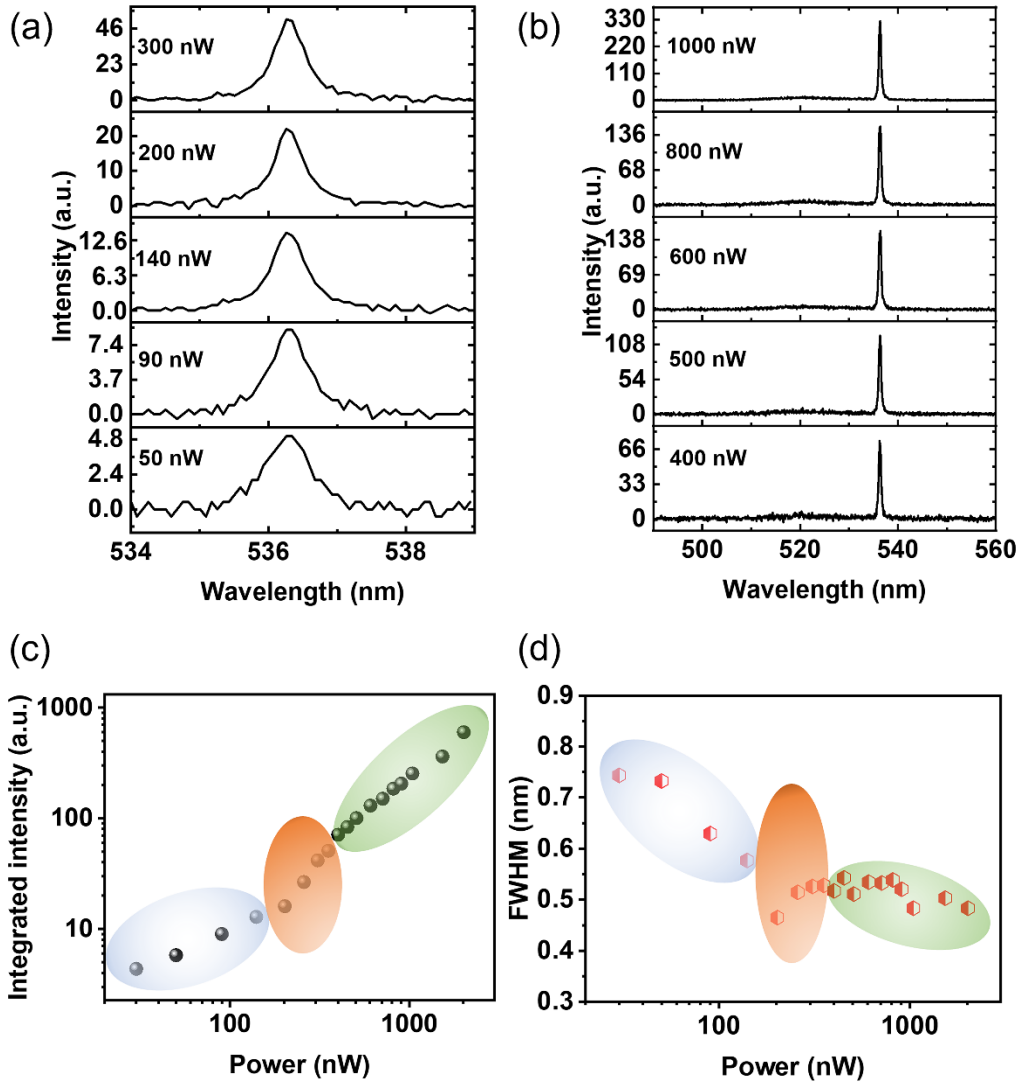

Figure S4 Lasing characterization of $CsPbBr_3$ QDs VSCEL after one-year preservation. (a) PL spectra collected at the small range under a variety of low excitation powers (≤ 300 nW). (b) PL spectra collected at the extensive range under a variety of excitation powers (≥ 400 nW). The intensity (c) and line width (d) of PL emission as a function of the excitation power. The light blue, orange, and green regions represent the spontaneous emission state, superlinear amplification state, and lasing emission state, respectively.

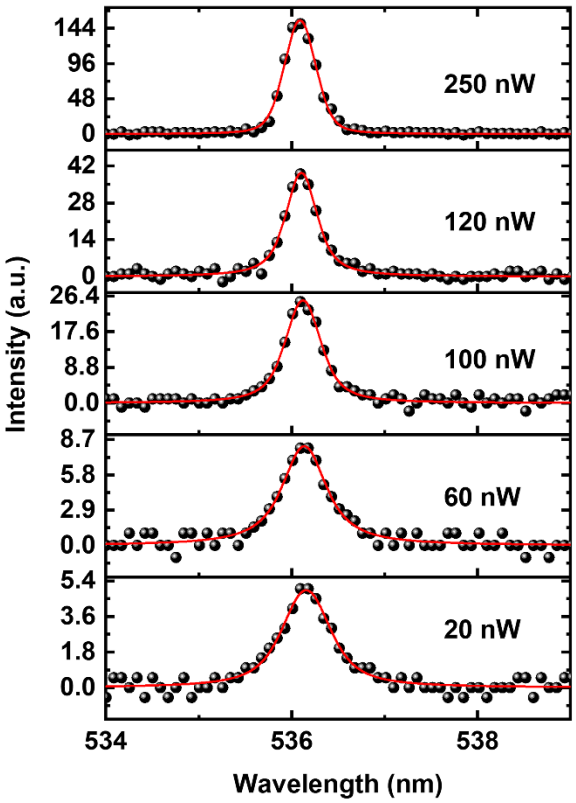

Figure S5 Photoluminescence spectra taken at low excitation powers (< 250 nW) and their fitting curves by Voigt function.

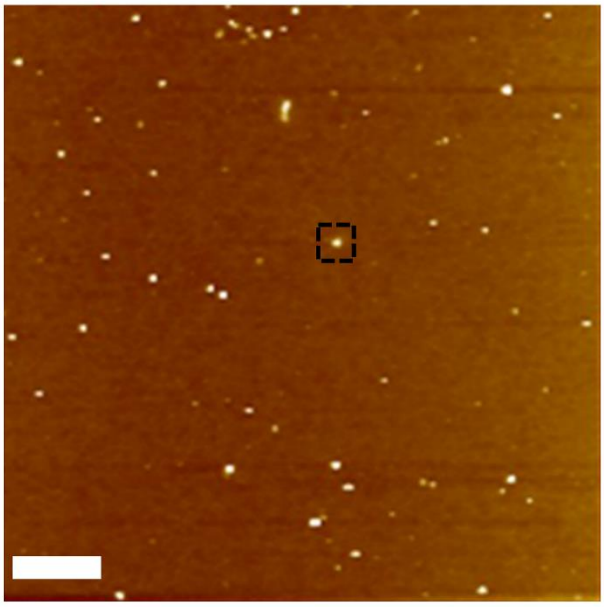

Figure S6 AFM image of $CsPbBr_3$ QDs spin-coated on DBRs for the spatial distribution. The CsPbBr3 QDs were in the same concentration as that of QDs embedded in a microcavity, which has been diluted enough to be isolated. Scale bar: 1μm. The marked region is zoomed-in and presented in Fig 1c.